

Twisted Tape Based Heat Transfer Enhancement In Parabolic Trough Concentrator – An Experimental study

D N Elton* U C Arunachala*

*Dept. of Mech. & Mfg. Engg, Manipal Institute of Technology, Manipal Academy of Higher Education, Manipal – 576104, Karnataka State, India

Email: *arun.chandavar@manipal.edu

Abstract. The heat transfer augmentation in parabolic trough concentrator is gaining importance now a days as it makes the system compact and efficient. Out of various techniques, use of twisted tape inserts is popular due to easy implementation as well as substantial enhancement in system performance. Most of the studies in this field pertaining to experimental/computational analysis with respect to both outdoor and indoor set ups. The rise in convective coefficient of heat transfer fluid due to insert has been studied by many researchers. But such studies are based on uniform heat flux or out-field non-uniform based which is under uncontrollable environment. Hence in the present study, Nusselt number correlations for plain absorber and absorber with twisted tape ($y=3.48$, 5.42 and 7.36) are developed under the realistic condition of solar concentration with controlled environment. The parity plot shows the maximum deviation of 20% which in turn indicates better quality of fit.

1. Introduction

Solar energy has been used by both nature and human kind throughout time in many ways. It is used to heat and cool buildings (both actively and passively), heat water for domestic and industrial uses, heat swimming pools, power refrigerators, operate engines and pumps, desalinate water for drinking purposes, generate electricity, for chemistry applications, and many more operations. Because of the desirable environmental and safety aspects it is widely believed that solar energy should be utilized instead of other conventional energy forms. Out of different applications of solar energy, the power generation by focusing type of collectors is gaining popularity now a days.

Parabolic trough power plants consist of large field of parabolic trough collectors (PTC), a heat transfer fluid/steam generation system, a Rankine steam turbine/generator cycle, and optional thermal storage and/or fossil-fired backup systems. The performance of PTC is based on optical and thermo-hydraulic configuration. Due to advanced optics technology presently in use, researchers have focused on performance enhancement of receivers taking into account various geometrical treatments.

2. Literature review

In this section, various heat transfer augmentation techniques applicable to PTC absorber have been highlighted.

An innovative flat aluminium absorber in small PTC for process heat and direct steam generation has been investigated by Bortolato et al. [1]. The absorber has got bar and plate technology



with an internal turbulator. Ray tracing was done to get the amount of flux in each bin using Soltrace®. Due to the high heat flux over the receiver a heat spreader is used to avoid hot spots on the surface and thus an offset turbulator has also been used inside the receiver to reduce the thermal gradient between the wall and the fluid. Due to low pressure drop, despite the presence of turbulator, makes it suitable for steam generation at even low mass flow rates. Jaramillo et al. [2] have worked on the thermal hydraulic performance of a PTC with twisted tape inserts for low enthalpy processes by considering the first and second law of thermodynamics for a temperature range of 70 to 110 °C. For the theoretical model, an empty tube and tube with twisted tape of twist ratio 2 was implemented and concluded that heat removal factor increases to 3 % and overall heat loss coefficient decreases by 1.5 % for twisted tape. For the numerical simulation, twist ratios of 1, 2, 3, 4 and 5 with Reynold number range of 1350 – 8350 was considered. The thermal efficiency increases as the twist ratio tends to 1, and as the flow rate increases the efficiency increases and thus get independent of the twist ratio at higher flow rates. The enhancement factor based on second law shows that for higher Reynold number and high twist ratios, there is no advantage of using twisted tape. It can thus be concluded that the best results are obtained only when twisted tapes are used for very low flow rates. Mwesigye et al. [3] numerically analyzed the effect of wall detached Twisted Tape having a twist ratio 0.5 – 2.0 for a turbulent range of Re (10260 – 1353000). Non-uniform heat flux boundary condition with heat flux extracted from Soltrace® was implemented along the circumference. Syltherm was considered as the HTF (Heat Transfer Fluid) in this analysis. Due to twisted tape 68% reduction in surface temperature and 1.05 – 2.69 times rise in Nu was noticed compared to plain tube. Further, Nu and f correlations were developed based on this results. Vashistha et al. [4] investigated the experimental use of single, double and 4 Twisted Tapes in co-swirl and counter-swirl (CT) orientations inside a tube having twist ratio 2.5, 3, 3.5 and Re in the range of 4000 - 14000. Better heat transfer rates are observed for lower Re with twisted tapes as there is a decline in performance with increasing Re. There is broadening of centrifugal forces and thus turbulent intensity near the wall when twist ratio is reduced. Counter swirl flow generates increasing whirl velocity thus 4CT perform the best at $y = 2.5$ compared to other configurations. In the thermo-hydraulic performance analysis, the 4CT surpass all the other configurations in complete Re range which is 1.23 - 1.26. The correlation for Nu and lie in the range of $\pm 4\%$ and $\pm 7\%$ respectively. Similar studies were performed by Song et al. [5], Waghole et al. [6], Ghadirijafarbeiglloo et al. [7] and Zhu et al. [8].

The influence of various fin configurations on the system performance were studied by Bellos et al. [9], [10], [11] and Xiangtau et al. [12]. All these studies have proved the enhancement in heat transfer rate at the cost of additional pressure drop.

Reddy et al. [13], Jamal-Abad et al. [14], Ghasemi and Ranjbar [15] and Wang et al. [16] have used different porous media and justified its role in the heat transfer augmentation. Apart from above mentioned techniques, other receiver surface treatment techniques were discussed by Fuqiang et al. [17], [18] and Jianseng et al. [19].

An intensive review mentions the benefit of performance augmentation with reference to experimental and/or computational analysis. Till date studies have been focused on uniform heat flux based indoor set up. Also, out-field experimental study or non-uniform heat flux based computational analysis have been tried. Hence in the present study, the non-uniform heat flux is simulated (with the use of Soltrace®) in case of indoor based receiver. Further, Nu correlation for the case of plain receiver as well as twisted tape is also developed.

3. Heat transfer augmentation in PTC

A cross-section of a parabolic trough collector is shown in Figure 1, the procedure for determining total heat loss from the receiver is discussed below. The convective heat transfer coefficient between glass cover and surrounding is,

$$h_{c,c-a} = \frac{Nu_{wind} \times k}{d_{go}} \text{-----(1)}$$

Similarly, convective heat transfer coefficient between receiver and cover is determined by,

$$h_{c,r-c} = \frac{2k_{eff}}{d_o \ln\left(\frac{d_{gi}}{d_o}\right)} \text{ where, } \frac{k_{eff}}{k} = 0.317(Ra^*)^{1/4} \quad (2)$$

The radiation heat loss coefficient from the glass cover outer surface to ambient is given by,

$$h_{r,c-a} = \varepsilon_g \sigma \left((T_g + 273) + (T_s + 273) \right) \times \left((T_g + 273)^2 + (T_s + 273)^2 \right) \quad (3)$$

The receiver – cover based radiation heat loss coefficient is:

$$h_{r,r-c} = \frac{\sigma \left((T_g + 273) + (T_r + 273) \right) \times \left((T_g + 273)^2 + (T_r + 273)^2 \right)}{\frac{1}{\varepsilon_r} + \frac{A_r}{A_g} \left(\frac{1}{\varepsilon_g} - 1 \right)} \quad (4)$$

Considering the both convective and radiative heat loss from the absorber surface and glass cover outer surface, the overall heat loss coefficient (U_L) is calculated as,

$$U_L = \left[\frac{A_r}{(h_{c,c-a} + h_{r,c-a}) A_g} + \frac{1}{(h_{r,r-c} + h_{c,r-c})} \right]^{-1} \quad (5)$$

Similarly, the overall heat transfer coefficient based on the outer surface area of the receiver,

$$U_o = \left[\frac{1}{U_L} + \frac{d_o}{d_i} \times \frac{1}{h_{fi}} + \frac{d_o \ln\left(\frac{d_o}{d_i}\right)}{2k_{abs}} \right]^{-1} \quad (6)$$

In equation (6), U_o can be raised by increasing h_{fi} as rest all parameters (except U_L) remains unchanged. However, U_L is inversely proportional to h_{fi} . Hence different methods are used to enhance h_{fi} .

The twisted tape (Figure 2) insert partially blocks the flow passage and also induces secondary swirl motion which increases the degree of turbulence of HTF. Simultaneously, the velocity of the HTF also increases due to the reduction in free flow area due to insertion of twisted tape. The combined effect of all these results in enhancement of useful heat gain by HTF.

The geometry of the twisted tape is specified by twist ratio which is defined as the ratio of the pitch length for 180° twist (H) to the width of the twisted tape (D). In general, the intensity of swirl is higher for lower twist ratios. In the present work, twisted tapes ($y = 3.48, 5.42$ and 7.36) are used.

The steps involved in the analysis with twisted tapes is similar to that of plain receiver except the following changes.

Free flow area in the receiver,

$$A_c = \frac{\pi}{4} d_i^2 - \delta D \quad (7)$$

$$\text{Mass velocity of HTF, } G = \frac{\dot{m}}{\left(\frac{\pi d_i^2}{4} - \delta D \right)} \quad (8)$$

Swirl velocity component,

$$V_s = \left(G / \rho \right) \sqrt{1 + \left(\pi / 2y \right)^2} \quad (9)$$

Reynold number based on swirl velocity component,

$$Re_s = \frac{\rho V_s d_i}{\mu} \quad (10)$$

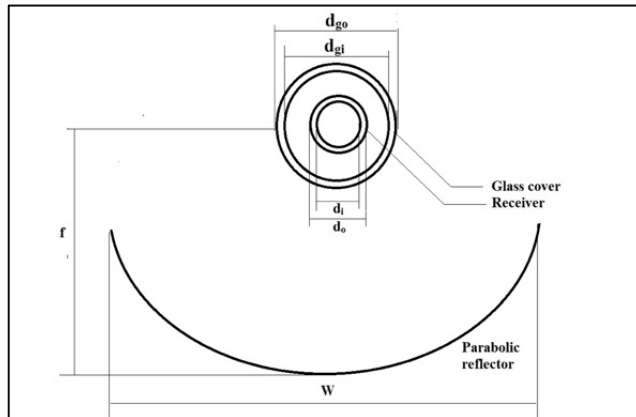


Figure 1: Specification of PTC

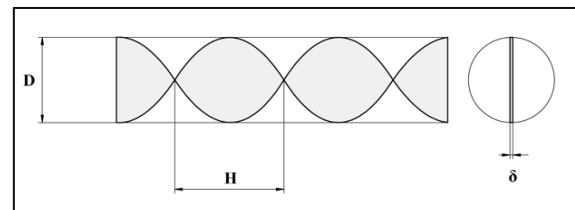


Figure 2: Longitudinal section of twisted tape

4. Experimental Analysis

For the detailed analysis, Soltrace® based solar radiation is taken as input to the receiver and Nu correlations are developed for the wide range of Re (2300 - 25000) with respect to different twisted tape inserts. The experiment is carried out for flow rates of 7, 13, 16, 19, 22, 25, 28 and 30 LPM. The day wise profile for the solar radiation, wind velocity, ambient temperature is taken as follows from the weather forecast report available from the MNRE website [20] for the area Manipal which is used in the heat loss calculation analytically and then that amount of solar radiation reduced is fed to the heating strips.

4.1 Experimental Setup

The experimental set up consists of test section, entry length, pumping unit, thermostatic bath, cooling unit, electrical components and measuring instrumentation units as shown in the schematic (Figure 3). The HTF (Therminol VP-1) in thermostatic bath can be circulated in the flow at pre-set temperature by means of gear pump. The flow fully develops in the entry length section before the test section. The required concentrated heat flux is provided to the HTF in the test section using differential heating of 6 Nichrome strips wound over the receiver. The HTF coming out of the test section is cooled in a crimped finned tube DPHX before entering the thermostatic bath. The test section is properly insulated to avoid the heat loss to surrounding. The output from 20 thermocouples (16 on receiver, HTF entry and exit temperature, insulation surface and ambient temperature), differential pressure transducer and flow meter are connected to data logger. Digital voltmeter and ammeter are used for the electrical power measurement.

4.2. Experimental procedure

In this section, the detailed experimental procedure for determining the energy parameters of PTC with plain tube/twisted tape insert is discussed. The experimental procedure for plain receiver as well as twisted tape inserts is nearly similar. However, additional steps involved in experimentation with twisted tape inserts are discussed.

- i. Required entry temperature of the HTF and flow rate are set in thermostatic bath and variable frequency drive.
- ii. During HTF flow, air bubbles are removed in the line with the help of valves.
- iii. Based on Soltrace® output, required electrical power is supplied to different Nichrome strips with the help of step down transformers and dimmer stats.
- iv. Once the system attains steady state, all readings are recorded.
- v. The above steps are repeated for the case of twisted tapes.

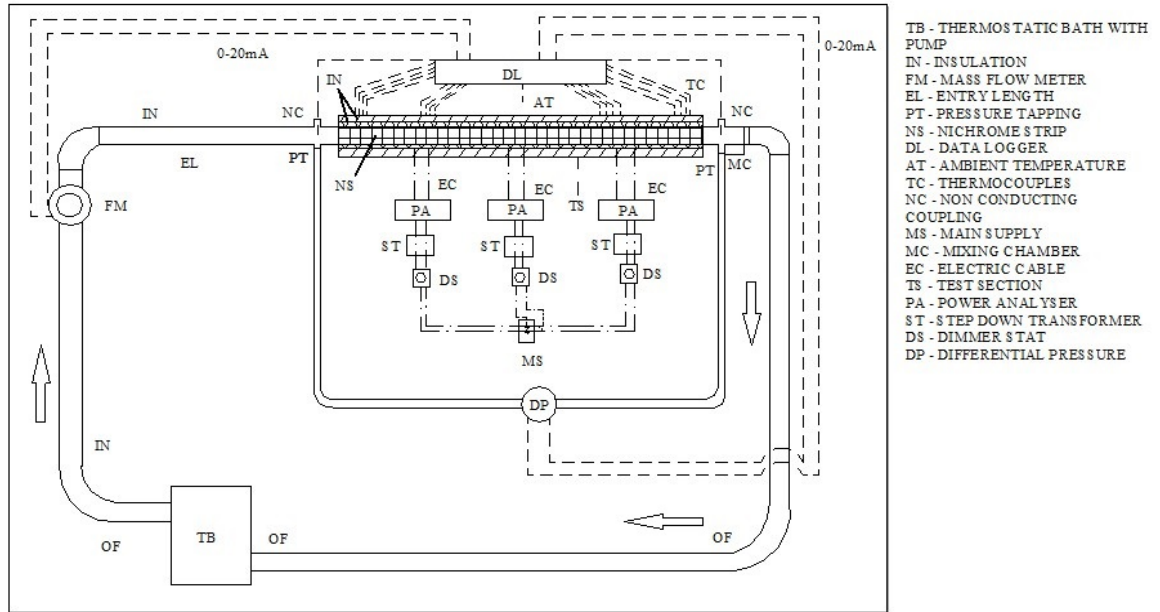


Figure 3. Schematic sketch of the experimental set up

4.3. Experimental data reduction

The method for deducing various energy parameters (through MATLAB) from experimental data is discussed below.

The mass flow rate of HTF is obtained from the volumetric flow rate as,

$$\dot{m} = \frac{\dot{q} \times \rho \times 10^{-3}}{60} \quad (11)$$

Mean temperature of HTF,

$$T_{m,exp} = \frac{T_{fi,exp} + T_{fo,exp}}{2} \quad (12)$$

Inner surface area of the receiver,

$$A_i = \pi d_i L \quad (13)$$

Useful heat gain by HTF,

$$Q_{u,exp} = \dot{m} c_p (T_{fo,exp} - T_{fi,exp}) \quad (14)$$

Inner surface temperature of the receiver,

$$T_{ri,exp} = T_{r,exp} - \left\{ \frac{Q_{u,exp} \times \ln\left(\frac{d_o}{d_i}\right)}{2 \times \pi \times k_r \times L} \right\} \quad (15)$$

Log mean temperature difference,

$$LMTD = \frac{\Delta T_1 - \Delta T_2}{\ln\left(\frac{\Delta T_1}{\Delta T_2}\right)} \quad (16)$$

Convective heat transfer coefficient of the HTF,

$$h_{fi,exp} = \frac{Q_{u,exp}}{A_i \times LMTD} \quad (17)$$

Experimental Nusselt number,

$$N_{u,exp} = \frac{h_{fi,exp} \times d_i}{k} \quad (18)$$

The error involved in the analysis is based on the accuracy of different instruments (Table 1)

The Soltrace® output as given in Figure 4 shows the solar ray distribution about the receiver after passing through a vacuum glass tube. The entire receiver tube is divided into 8 bins and the solar radiation falling on it is averaged about that particular bin over the length. With this distribution, the Local Concentration Ratio (LCR) about the receiver is found and cross multiplied for corresponding solar radiations in W/m². Later this radiation value is used as an input (resistance heating) to the test section.

Table 1: Error in the measuring instruments

Instrument	Error
Thermocouple connected to data logger	± 0.001°C
Flow meter	±0.1 LPM
Multimeter	±0.01 W
Differential pressure transducer	±1 Pa

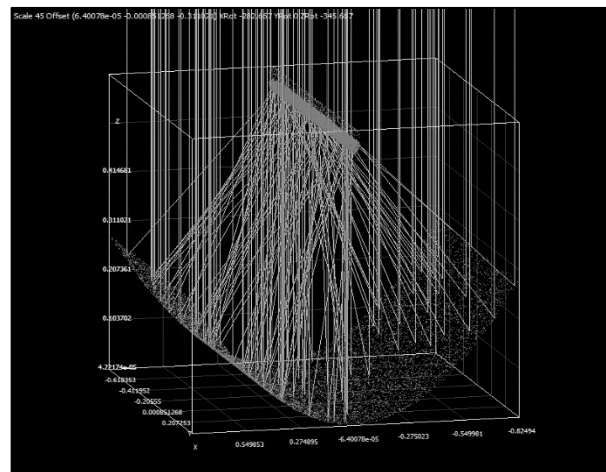


Figure 4: Visualization of solar ray path in Soltrace®

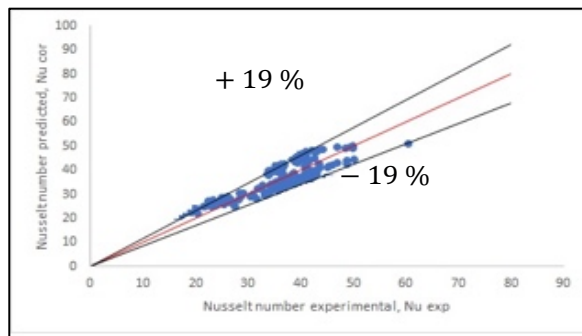
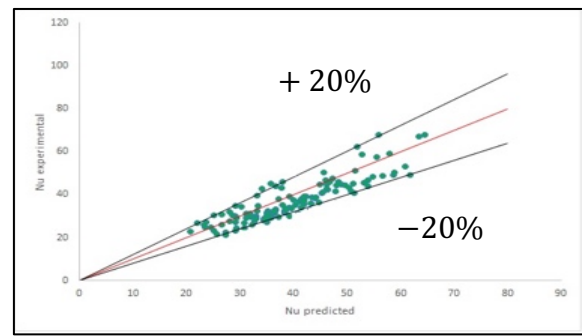
5. Results and discussion

As there is no Nu correlations available for non-uniform heat flux applicable to plain tube as well as tube with twisted tape inserts the following result highlights its importance mainly for DNI based applications.

The experiment was conducted with varying inlet conditions (Inlet temperature from 40 – 100 °C, DNI of 167 – 671 W/m² and flow rate of 7 – 30 lpm) to determine experimental Nu . The Nusselt number for plain tube from literature review was found to be of the form $Nu = CRe^m Pr^n$. By using regression analysis, the coefficients of C , m and n are found out. These coefficients are then minimized by reducing the error generated by subtracting predicted Nu from experimental Nu . This way the Nusselt number correlation for plain tube was found. Figure 5 shows the parity plot of Nusselt number predicted vs Nusselt number experimental for plain tube and lies in the range of ± 19% of experimental Nusselt number. The range of Re (2300 – 25000) covered is from the transition range to turbulent region. The laminar and sub laminar region haven't been covered in the present work due to difficulties in experimental operation. The predicted Nusselt number is,

$$Nu = 0.25Re^{0.48}Pr^{0.17} \quad (19)$$

The Nusselt number was plotted also for plain tube with twisted tape inserts and a generalized correlation with twist ratio ($y = 3.48 - 7.36$) being the independent term present in the equation. The correlations developed so far has the averaged surface flux. In the present work the heat flux was divided into 6 parts having symmetric heat flux about the centre. From the literature review the

Figure 5: Parity plot of Nu for plain tubeFigure 6: Parity plot of Nu for tube with twisted tape

Nusselt number correlation was found to be the best of the form $Nu = CPr^m(Res/y)^n$. The other forms of Nu weren't in well agreement with the experimental data and had a high range of error. The same procedure as mentioned earlier was followed to find the Nusselt number experimentally and then predicted for the experimental data. There error in Nu predicted lies in between $\pm 20\%$. The predicted Nusselt number for twisted tapes was thus found to be:

$$Nu = 1.21Pr^{0.127}(Res/y)^{0.406} \text{-----} (20)$$

6. Conclusion

The heat transfer enhancement in PTC due to twisted tape inserts has been studied. The primary objective was to develop Nu correlations for plain absorber as well as absorber with twisted tape under realistic non-uniform solar radiation level. This was done by taking good number of data points. From parity plots it has been observed that both the correlations are matching with an error less than 20%. Hence for PTC analysis, the present correlation is more viable than the uniform heat flux based Nu correlations.

Nomenclature

A	Area [m ²]
C	Geometrical concentration ratio [-]
D	Width of twisted tape [m]
d	Diameter [m]
H	Twisted tape pitch for 180° twist [m]
I	Solar beam radiation intensity [W/m ²]
k	Thermal conductivity [W/mK]
L	Length [m]
\dot{q}	Volume flow rate of HTF (LPM)
T	Temperature [°C]
y	Twist ratio [-]

Subscripts:

a	ambient, aperture
exp	experimental values
f	flowing fluid
fi	HTF inlet
fo	HTF outlet

g	glass cover
gi	glass cover inner surface
go	glass cover outer surface
i	instantaneous, inner
m	bulk mean
r	receiver
s	sky

Greek symbols:

μ	Absolute viscosity [Ns/m ²]
α	Absorptivity of receiver
ρ	Density [kg/m ³], reflectance of the mirror
ε	Emissivity, surface roughness factor
σ	Stefan-Boltzmann constant [5.67×10 ⁻⁸ W/m ² K ⁴]
τ	Transmissivity of glass cover
δ	Twisted tape thickness [m]

References

- [1] Bortolato, M., Dugaria, S. and Col, D., D., 2016. Experimental study of parabolic trough collector with flat bar-and-plate absorber during direct steam generation, Energy, 116, 1039-1050.

- [2] Jaramillo, O., A., Borunda, M., Velazquez-Lucho, K., M. and Robles, M., 2016. Parabolic trough collector for low enthalpy processes: An analysis of the efficiency enhancement by using twisted tape inserts, *Renewable energy*, 93, 125- 141.
- [3] Mwesigye, A., Bello-Ochende, T. and Meyer, J., P., 2016. Heat transfer and entropy generation in a parabolic trough receiver with wall-detached twisted tape inserts, *International Journal of thermal science*, 99, 238-257.
- [4] Vashistha, C., Patil, A., K. and Kumar, M., 2016. Experimental investigation of heat transfer and pressure drop in a circular tube with multiple inserts, *applied thermal engineering*, 96, 117-129.
- [5] Song, X., Dong, G., Gao, F., Diao, X., Zheng, L. and Zhou, F., 2014. A numerical study of parabolic trough receiver with nonuniform heat flux and helical screw-tape inserts, *Energy*, 77, 771-782.
- [6] Waghole, D., R., Warkhedkar, R., M., Kulkarni, V., S. and Shrivasta, R., K., 2014. Experimental investigations on heat transfer and friction factor of silver nanofluid in absorber/receiver of parabolic trough collector with twisted tape inserts, *Energy procedia*, 45, 558 - 567.
- [7] Ghadirijafarbeigloo, Sh., Zamzamin, A., H. and Yaghoubi, M., 2014. 3-D numerical simulation of heat transfer and turbulent flow in a receiver tube of solar parabolic trough concentrator with louvered twisted-tape inserts, *Energy procedia*, 49, 373 – 380.
- [8] Zhu, X., Zhu, L. and Zhao, J., 2017. Wavy-type insert designed for managing highly concentrated solar energy on absorber tube of parabolic trough receiver, *Energy*, 141, 1146 – 1155.
- [9] Bellos, E., Tzivanidis, C. and Tsimpoukis, D., 2017. Thermal enhancement of parabolic trough collector with internally finned absorbers, *Solar energy*, 157, 514 – 531.
- [10] Bellos, E., Tzivanidis, C., Daniil, I. and Antonopoulos, K., A., 2017. The impact of internal longitudinal fins in parabolic trough collectors operating with gases, *Energy conversion and management*, 135, 35 – 54.
- [11] Bellos, E., Tzivanidis, C. and Tsimpoukis, D., 2017. Multi-criteria evaluation of parabolic trough collector with internally finned absorbers, *Applied Energy*, 205, 540 - 561.
- [12] Xiangtao, G., Fuqiang, W., Haiyan, W., Jianyu, T., Qingzhi, L. and Huaizhi, H., 2017. Heat transfer enhancement analysis of tube receiver for parabolic trough solar collector with pin fin arrays inserting, *Solar Energy*, 144, 185 – 202.
- [13] Reddy, K., S., Kumar, K., R. and Ajay, C., S., 2015. Experimental investigation of porous disc enhanced receiver for solar parabolic trough collector, *Renewable Energy*, 77, 308-319.
- [14] Jamal-Abad, M., T., Saedodin, S. and Aminy, M., 2017. Experimental investigation on a solar parabolic trough collector for absorber tube filled with porous media, *Renewable Energy*, 107, 156 – 163.
- [15] Ghasemi, S., E. and Ranjbar, A., A., 2017. Numerical thermal study on effect of porous rings on performance of solar parabolic trough collector, *Applied Thermal Engineering*, 118, 807 – 816.
- [16] Wang, P., Liu, D., Y. and Xu, C., 2013. Numerical study of heat transfer enhancement in the receiver tube of direct steam generation with parabolic trough by inserting metal foams, *Applied energy*, 102, 449 – 460.
- [17] Fuqiang, W., Qingzhi, L., Huazhi, H. and Jianyu, T., 2016. Parabolic trough receiver with corrugated tube for improving heat transfer and thermal deformation characteristics, *Applied energy*, 164, 411 – 424.
- [18] Fuqiang, W., Zhexiang, T., Xiangtao, G., Jianyu, T. and Huaizhi, H., 2016. Heat transfer performance enhancement and thermal strain restrain of tube receiver for parabolic trough solar collector by using asymmetric outward convex corrugated tube, 114, 275 – 292.
- [19] Jianfeng, L., Xiangyang, S., Jing, D. and Jianping, Y., 2013. Transition and turbulent convective heat transfer of molten salt in spirally grooved tube, *Experimental thermal and fluid science*, 47, 180 – 185.
- [20] <http://mnre.gov.in/sec/solar-assmnt.htm>, solar radiation data, 01/06/2016